International Journal of Innovation in Mechanical Engineering and Advanced Materials
Homepage: publikasi.mercubuana.ac.id/index.php/ijimeam
Vol. 8 (No. 2), 2024, pp. 130-143
DOI: 10.22441/ijimeam.v8i2.38546

Demineralization of Silica-Rich Agar Processing Residues via Hydrofluoric Acid Leaching for Organic Fraction Enrichment

Andi F. Sudarma [1,2], Edy Hartulistiyoso [1,4,*], Y. Aris Purwanto [1], Leopold O. Nelwan [3,4], Obie Farobie [1,5], Hendri [6], Harri Junaedi [7], and Edy H. Majlan [8]

[1]Department of Mechanical and Biosystem Engineering, IPB University, Bogor 16680, Indonesia
[2]Department of Mechanical Engineering, Universitas Mercu Buana, Jakarta 11650, Indonesia
[3]Division of Biosystem Engineering, IPB University, Bogor 16680, Indonesia
[4]Center for Research on Engineering Application in Tropical Agriculture (CREATA), IPB University, Bogor 16680, Indonesia
[5]Surfactant and Bioenergy Research Center (SBRC), IPB University, Bogor 16143, Indonesia
[6]Department of Mechanical Engineering, Institut Teknologi PLN, Jakarta 11750, Indonesia
[7]Department of Engineering Management, Prince Sultan University, Riyadh 12435, Saudi Arabia
[8]Fuel Cell Institute, Universiti Kebangsaan Malaysia, Selangor 43600, Malaysia
*Corresponding Author: edyhartulistiyoso@apps.ipb.ac.id (EH)

Abstract

Agar solid waste (ASW) is a silica-rich industrial residue generated during agar extraction that contains organic residue mixed with mineral filtration aids such as Celite (diatomaceous earth) and perlite. Its high ash content and low organic fraction limit its direct utilization as a biomass-derived fuel. This study investigated hydrofluoric acid (HF) leaching as a demineralization pretreatment to reduce silica-rich minerals and improve the physicochemical quality of ASW. Two ASW samples obtained from different agar-processing plants, namely ASW-Celite (contain Celite) and ASW-Perlite (contain perlite), were treated using 10 wt% HF at a solid-to-liquid ratio of approximately 1:12. The treated samples were characterized using XRF, ICP-MS, FTIR, ultimate analysis, and proximate analysis. HF leaching caused substantial mass reduction, with solid yields of 24.99% for ASW-Celite-HF and 48.9% for ASW-Perlite-HF. Ash content decreased from 85.84 to 44.99 wt% in ASW-Celite and from 77.10 to 24.83 wt% in ASW-Perlite. XRF analysis confirmed significant silica removal, particularly in ASW-Celite, where SiO_2 decreased from 96.94 to 21.30%. ICP-MS further showed the reduction of several ash-forming and environmentally relevant elements, including Cr, Ni, Cu, Zn, Cd, P, S, Cl, Mn, and Fe. HF treatment also enriched the organic fraction, increasing carbon content from 4.69 to 12.52 wt% in ASW-Celite and from 9.83 to 16.10 wt% in ASW-Perlite. The HHV of ASW-Celite improved from 1.91 to 6.52 MJ/kg, whereas ASW-Perlite decreased from 4.80 to 3.19 MJ/kg due to its high oxygen content after treatment. These findings demonstrate that HF leaching effectively reduces silica-rich minerals in ASW, although further deoxygenation is required to improve its fuel quality for bioenergy applications.

Article Info:
Received: 27 March 2026
Revised: 27 June 2026
Accepted: 30 June 2026
Available online: 21 August 2026

Keywords:
agar solid waste; hydrofluoric acid leaching; demineralization; ash content; biomass; ICP-MS

How to cite:

A. F. Sudarma, E. Hartulistiyoso, Y. A. Purwanto, L. O. Nelwan, O. Farobie, Hendri, H. Junaedi, and E. H. Majlan, "Demineralization of silica-rich agar processing residues via hydrofluoric acid leaching for organic fraction enrichment," *Int. J. Innov. Mech. Eng. Adv. Mater.*, vol. 8, no. 2, pp. 130–143, 2026.

1. Introduction

Agar production from *Gracilaria* macroalga constitutes a major marine biomass industry and generates substantial quantities of solid residues. According to FAO statistics, global production of agar seaweed reached 3,695,231 wet tons in 2019. In Indonesia, agar production was estimated to reach 180–550 tons per year in 2020, reflecting the significant scale of industrial processing and the associated waste generation [1]. Despite its economic importance, the agar extraction process exhibits relatively low biomass utilization efficiency, with only 17–43% of the raw macroalga converted into agar, while approximately 60–75% remains as solid residue [1], [2]. This agar solid waste (ASW) contains cellulose, hemicellulose, and residual agar, making it a potentially valuable biomass resource for energy and material applications [1], [3], [4]. However, despite its considerable organic content, ASW remains largely underutilized. Improper disposal can lead to waste accumulation, odor generation, and operational challenges for processing facilities [5], [6], [7], [8]. Therefore,

Table 1. HF-sensitive elements that are commonly found in minerals and soil.

Sensitivity to HF	Elements	Why they are sensitive
Very high	Si, Al	HF strongly attacks silica, glass, silicates, aluminosilicates, Celite, perlite, clay-like phases [15], [16], [17]
High	Ti, Zr, Hf, Nb, Ta, W	Form stable fluoride or oxyfluoride complexes; often affected during HF digestion/leaching [18], [19]
High	B, Ge, Sn	Can form volatile or soluble fluorinated species; may decrease or behave irregularly [20]
Moderate–high	Ca, Mg, Sr, Ba	Can form poorly soluble fluorides, e.g., CaF_2, MgF_2, BaF_2; may precipitate instead of dissolve [21]
Moderate–high	La, Ce, Nd, Sm, Gd, Dy, Y, Yb, Lu	Rare earth elements can form insoluble fluoride precipitates; may become enriched in the residue [22], [23], [24]
Moderate	Th, U	Can form fluoride complexes or precipitated fluoride species; may concentrate in solid residue [25]
Moderate	Fe, Mn, Cr, Ni, Co, Cu, Zn	Can dissolve partly, but response depends on mineral form and redox/speciation [26]

developing effective strategies to recover and utilize the remaining biomass is essential for improving resource efficiency and supporting a circular bioeconomy within the agar-processing sector.

The limited utilization of ASW is primarily attributed to its exceptionally high inorganic content. Unlike most lignocellulosic residues, the mineral fraction of ASW is not solely derived from the biomass itself but is substantially increased by the addition of filtration aids during agar extraction. Celite (diatomaceous earth) and perlite are commonly used to improve filtrate clarity and prevent filter clogging [9], [10]. Both materials are highly siliceous, containing approximately 85–90 wt% and 70–75 wt% SiO_2, respectively [11], [12], [13]. Consequently, ASW may contain ash levels as high as 59.18–78.75 wt%, significantly exceeding those of conventional biomass feedstocks [1]. Such high silica concentrations are particularly problematic because silica remains thermally stable during combustion and thermochemical conversion, resulting in low heating values, increased slagging and fouling tendencies, and reduced process efficiency [14]. Therefore, the challenge in valorizing ASW is not merely reducing ash content, but selectively removing silica-rich mineral phases while preserving the organic fraction.

Previous studies have shown that washing and acid pretreatment can reduce inorganic species and improve fuel properties, although the effectiveness depends strongly on biomass type, mineral form, and treatment severity [27], [28]. Mechanical approaches such as multistage grinding and sieving have successfully reduced ASW ash content to 8.27 wt% [10]. However, their effectiveness depends on the physical liberation of mineral particles and becomes limited when inorganic components are strongly attached to or embedded within the fibrous matrix. In industrial ASW, filtration aids are often subjected to mechanical compression during filtration, promoting intimate contact between siliceous particles and organic fibers, as reported in [29]. Under such conditions, physical separation alone may be insufficient to achieve substantial demineralization. Chemical pretreatment offers a more promising alternative because it targets mineral phases directly and is less dependent on particle liberation.

Acid leaching has been widely applied to remove inorganic constituents from silica-rich biomass. Various acids, including HF (hydrofluoric acid), HCl (hydrochloric acid), H_2SO_4 (sulfuric acid), H_3PO_4, HI, and citric acid ($C_6H_8O_7$), have been investigated for demineralization purposes [30]. HCl is frequently reported as an effective deashing agent and can produce silica purities of 91–99% from rice-husk-derived silica [30]. Likewise, H_2SO_4 treatment has improved the fuel properties of sewage sludge and wastewater algae by reducing ash content and increasing higher heating value [14], [31]. For ASW, HCl treatment has been reported to decrease ash content from 68.44% to 56.91% [32]. Nevertheless, these studies primarily focus on general deashing rather than selective silica removal. Since silica is the dominant inorganic component in ASW, conventional mineral acids may be insufficient to achieve deep demineralization. [14], [30], [31].

In contrast, HF possesses a unique ability to dissolve silicate structures through the formation of soluble fluorosilicate complexes [33], [34]. This property makes HF substantially more effective for silica removal than conventional mineral acids. Table 1 shows some

elements and its reactivity to HF during leaching process. HF was selected because of its strong affinity toward silica-rich minerals. During the demineralization process, silica reacts with HF to form soluble fluorosilicate species according to:

$$SiO_2 + 6HF \rightarrow 2H_2O + H_2SiF_6 \quad (1)$$

where the formation of soluble fluorosilicate compounds facilitates the removal of silica from the solid matrix during filtration and washing.

Previous studies reported silicon removal efficiencies of up to 99.47% from titanium dioxide powder [35], while HF achieved 98.2% silicate mineral removal from coal compared with only 52.9% for HCl under comparable conditions [36]. Despite its demonstrated effectiveness toward silica-rich materials, the application of HF for upgrading ASW has not been systematically investigated. Furthermore, no study has compared the demineralization behavior of ASW containing different filtration aids, despite the substantial differences in mineralogy between Celite and perlite.

Despite its high effectiveness for silica dissolution, the application of HF raises important environmental and safety concerns. HF is highly corrosive and toxic, posing significant risks to human health and the environment if not handled, stored, and disposed of properly [37]. Consequently, its industrial use requires stringent safety protocols, specialized equipment, and appropriate waste-treatment systems, which may increase operational complexity and cost. In contrast, hydrochloric acid (HCl) is generally considered safer and easier to handle and is therefore more commonly employed in biomass demineralization processes. However, while HCl is effective for removing many inorganic impurities, its ability to dissolve silica-rich minerals is substantially lower than that of HF [35]. This creates a trade-off between process safety and demineralization efficiency, particularly for silica-dominated residues such as ASW. Therefore, evaluating the effectiveness of HF for selective silica removal is important to determine whether the improvement in biomass quality justifies the additional safety and environmental considerations associated with its use.

Moreover, a critical knowledge gap remains regarding the selective removal of silica-rich minerals from ASW and the extent to which filtration aid mineralogy governs demineralization efficiency and the subsequent enrichment of the organic fraction. To address this gap, the present study systematically evaluates the effectiveness of HF leaching as a selective demineralization strategy for ASW containing two mineralogically distinct filtration residues: Celite-derived amorphous silica (ASW-Celite) and perlite-derived aluminosilicate phases (ASW-Perlite). Changes in ash forming element concentration, ash content, elemental composition, functional group characteristics, and higher heating value (HHV) were quantified before and after HF treatment to assess the extent of mineral removal and organic enrichment in each sample type.

2. Methods

Demineralization of ASW was performed through HF leaching to selectively remove silica-rich mineral phases and enhance the organic fraction. The overall experimental procedure is illustrated in Figure 1.

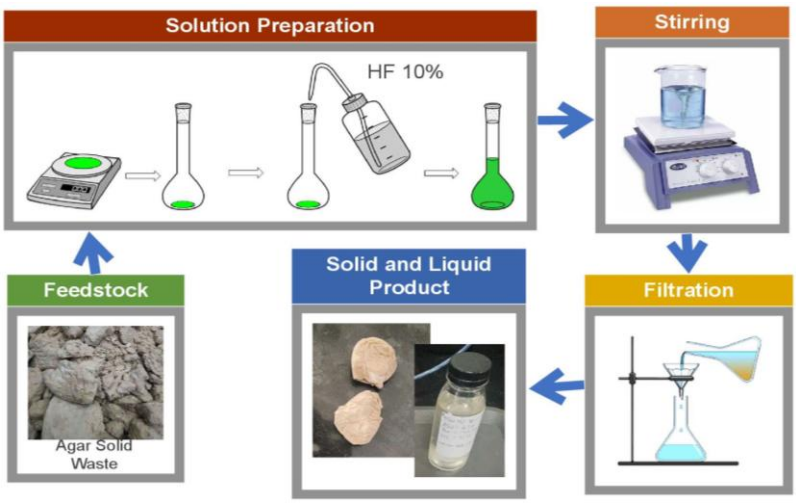

Figure 1. Schematic illustration of the ASW HF leaching (10% concentration) process.

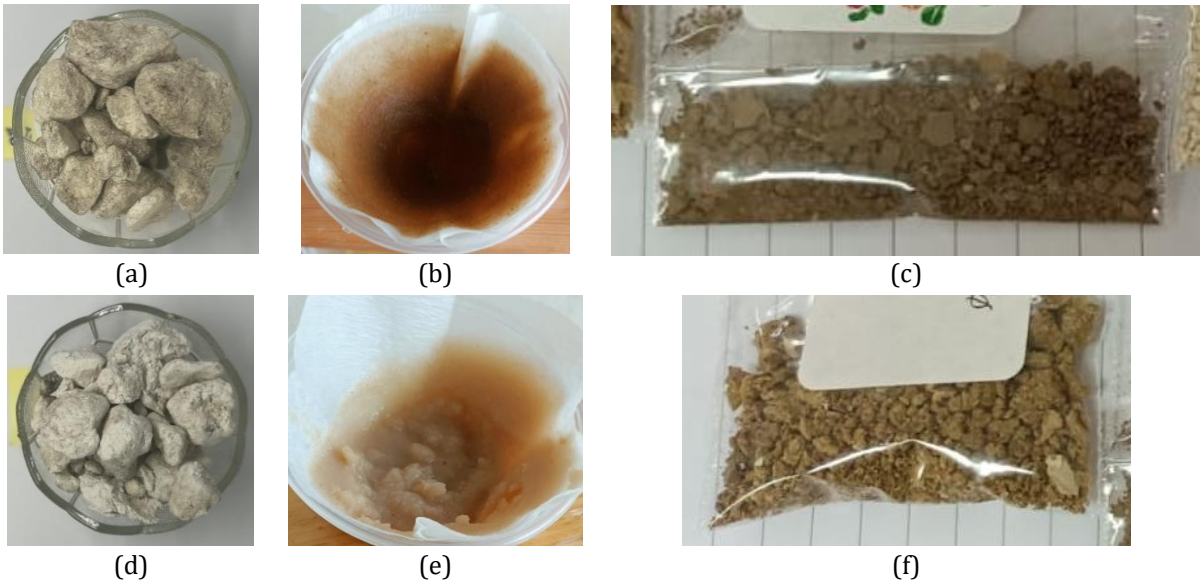

Figure 2. Solid waste from the agar extraction process and solid product after HF leaching (10% concentration; solid-to-liquid ratio of 1:12). Physical appearance of: (a) ASW-Celite before leaching, (b) ASW-Celite-HF during filtration, (c) ASW-Celite-HF solid product, (d) ASW-Perlite before leaching, (e) ASW-Perlite-HF during filtration, and (f) ASW-Perlite-HF solid product.

2.1. Sample preparation

ASW was obtained from two separate agar manufacturing facilities, referred to as ASW-Celite (from Plant A, located in Western Java, Indonesia) and ASW-Perlite (from Plant B, located in Eastern Java, Indonesia). These residues were byproducts of the filtration phase during agar production, comprising leftover biomass combined with filtration agents — specifically Celite in the case of ASW-Celite and perlite for ASW-Perlite. The gathered samples underwent open-air drying under natural sunlight for roughly 30 to 40 hours, spanning three to four days, until a consistent moisture level was reached. Throughout the drying process, the surrounding temperature stayed within the range of 30–35 °C, while relative humidity fluctuated between 60% and 80%. Once dried, the samples were kept in airtight containers until further processing. Visual representations of the untreated ASW samples can be found in Figure 2(a) and Figure 2(d).

A 10 wt% HF solution was prepared by mixing 41 mL of 40 wt% HF with 150 mL of distilled water; the HF used was produced by Merck. The HF concentration was selected based on the maximum concentration threshold considered acceptable under HF safety considerations, namely 10 wt%. Proper safety measures, including personal protective equipment (PPE), were implemented during this leaching process. For each experiment, 12.6 g of dried ASW was added to the solution, corresponding to a solid-to-liquid ratio of approximately 1:12 (w/w). All equipment used during this treatment was made of plastic. The suspension was stirred using a magnetic stirrer at ambient temperature. During the process, the suspension released heat due to the reaction. The heat was measured using a non-contact thermometer, and the reaction was considered complete when the temperature nearly reached ambient temperature.

Following leaching, the slurry was separated by filtration, as shown in Figure 2(b) and Figure 2(e). The solid residue was then dried in a laboratory oven at 105 °C until constant weight was achieved. The dried products were designated as ASW-Celite-HF and ASW-Perlite-HF, as shown in Figure 2(c) and Figure 2(f). The experiment was conducted with varying initial masses of ASW across 9 different mass values, as shown in Table 2. Two replicate samples were prepared for averaging the mass yield results, particularly for characterization purposes. Furthermore, an additional term was introduced to differentiate solid biomass before and after leaching, where ASW-Celite-HF and ASW-Perlite-HF represent the product yield after HF leaching.

2.2. Characterization

The initial and final solid masses of all samples subjected to HF leaching are summarized in Table 3. The effectiveness of the demineralization process was evaluated by determining the solid yield according to Equation (2).

Table 2. Initial mass variation of ASW samples and solid-to-liquid (S/L) ratio subjected to the HF leaching process for ASW-Celite and ASW-Perlite, arranged in ascending order.

	Initial Mass (g) of ASW before HF Leaching								
Sampel No.	1	2	3	4	5	6	7	8	9
ASW-Celite	12.64	15.80	18.73	20.30	21.93	22.72	23.50	25.06	28.20
S/L Ratio	1 : 11.86	1 : 9.49	1 : 8.01	1 : 7.39	1 : 6.84	1 : 6.6	1 : 6.38	1 : 5.98	1 : 5.32
ASW-Perlite	3.16	3.94	4.76	6.30	7.10	7.99	9.53	11.11	12.69
S/L Ratio	1 : 47.51	1 : 38.05	1 : 31.52	1 : 23.81	1 : 21.14	1 : 18.77	1 : 15.74	1 : 13.5	1 : 11.82

$$Solid\ Yield\ (\%) = {}^{m_{final}}/_{m_{initial}} \times 100\% \quad (2)$$

where m_{final} denotes the mass of the dried residue after leaching and $m_{initial}$ denotes the initial dry mass of the raw ASW.

Characterization was performed on one representative sample from each ASW type: ASW-Celite was represented by Sample No. 1, and ASW-Perlite was represented by Sample No. 9 in Table 2. The physicochemical properties of both raw and HF-treated samples were characterized using a suite of complementary analytical techniques. Elemental composition was determined by Inductively Coupled Plasma–Mass Spectrometry (ICP-MS; Perkin Elmer NexION 2000) and by X-ray Fluorescence (XRF; Bruker S2 PUMA) using the SMART-Oxides measurement method. Functional groups and structural changes in organic and inorganic components were examined by Fourier Transform Infrared Spectroscopy (FTIR; Shimadzu IRPrestige-21). Ultimate analysis (C, H, N, S, and O; Thermo Scientific FlashSmart CHNS/O) and proximate analysis were subsequently conducted. Proximate analysis provided the moisture content, volatile matter (VM), ash content, and fixed carbon (FC), all determined via thermogravimetric analysis (TGA). Measurement replication was performed automatically by the respective instruments, and results are reported as mean values.

ICP-MS data are reported as elemental concentrations in ppb. The element removal efficiency (%) was calculated using Equation:

$$Element\ removal\ eff. = \left[1 - {}^{C_{final} \times m_{final}}/_{C_{initial} \times m_{initia}}\right] \times 100\% \quad (3)$$

where C_{initial} and C_{final} denote the elemental concentrations (ppb) in the solid before and after HF treatment, respectively, and m_{initial} and m_{final} denote the corresponding solid masses.

The energy potential of the samples was assessed using the HHV. It was performed by combining ultimate and proximate analyses, with all results reported on a weight percentage basis. The oxygen content was calculated by difference according to: O (%) = 100% − (%C + %H + %N + %S + %Ash).

The HHV was estimated using the correlation proposed by Demirbas et al., based on the modified Dulong formula, as shown in Equation (4) [38].

$$HHV\ \left(\frac{MJ}{kg}\right) = 0.316 * C + 1.423 * H\ + 0.308 * S - 0.154 * O - 0.145 * N \quad (4)$$

where C, H, N, S, and O represent the elemental composition (wt%) on a dry basis.

3. Results and Discussion

A comprehensive evaluation of the physicochemical properties of ASW before and after HF leaching was conducted to assess the effects of demineralization on solid yield, elemental composition, functional groups, and energy characteristics. Particular attention was given to the high inorganic content of ASW, especially silica originating from filtration aids (Celite and perlite), to examine the extent to which HF treatment enhances the organic fraction.

The results are discussed in relation to structural changes identified by FTIR, compositional variations obtained from ICP-MS, XRF, CHNS and proximate analysis, and their implications for fuel properties based on proximate analysis and higher heating value (HHV). In addition, changes in elemental ratios are interpreted using the Van Krevelen diagram to elucidate the compositional evolution of ASW following demineralization.

3.1. Product yield

Figure 3 presents the relationship between the initial mass of ASW and the final solid residue obtained after HF leaching. Both ASW-Celite and ASW-Perlite exhibited strong positive linear correlations between the initial and final solid masses, indicating that the final residue mass was predominantly governed by the initial solid loading under conditions of constant HF concentration and solution volume.

The comparatively lower solid yield of ASW-Celite (Figure 3, top) suggests more effective dissolution of its inorganic fraction, which is consistent with the nature of Celite as the primary filtration aid. Celite is composed mainly of amorphous silica, a form that is highly reactive toward HF and readily converted into soluble fluorosilicate species. By contrast, ASW-Perlite (Figure 3, bottom) contains perlite-derived minerals, which are aluminosilicate-based and are expected to exhibit greater resistance to HF attack owing to their more complex crystalline structure. Accordingly, the higher final residue mass observed for ASW-Perlite reflects lower demineralization efficiency and greater retention of inorganic or mineral-associated material following treatment. The observed mass loss is therefore attributed primarily to chemical dissolution of inorganic constituents rather than to physical material loss, consistent with prior findings on HF-assisted ash removal in acid-leaching systems [39]. Notably, compared with previous studies in which acid leaching of various biomass feedstocks required several hours [14], [30], [31], the HF leaching process in the present study was completed in less than one hour, typically within approximately 45 minutes. An exothermic response was observed during the reaction, as evidenced by a rise in suspension temperature, and completion was indicated by the return of suspension temperature to near-ambient conditions.

The solid yield results, summarized in Table 3, confirm substantial mass removal during HF leaching. For ASW-Celite, the solid mass decreased from 12.64 g to 3.16 g, corresponding to a solid yield of 24.99%. For ASW-Perlite, the solid mass decreased from 12.70 g to 6.21 g, yielding a higher solid yield of 48.90%. This difference suggests that ASW-Celite underwent more extensive dissolution than ASW-Perlite under the same HF concentration and solid-to-liquid ratio.

3.2. XRF-based evaluation of mineral redistribution after HF leaching

XRF analysis was employed to evaluate the inorganic oxide distribution in raw and HF-treated ASW-Celite, as presented in Figure 4. The analysis provides informative data on major ash-forming elements — particularly Si, Al, K, Ca, Fe, P, S, and Cl — which are of direct relevance to biomass demineralization and bioenergy applications.

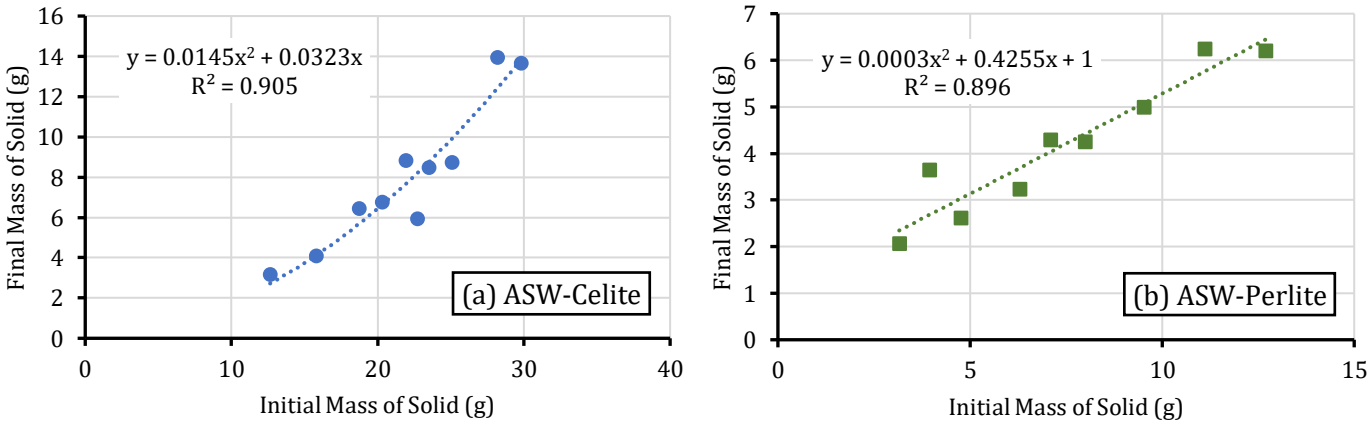

Figure 3. Relationship between the initial mass of ASW and the final solid residue after HF leaching (with 150mL 10% HF concentration) for (a) ASW-Celite and (b) ASW-Perlite.

Table 3. Solid yield following the HF leaching process (10% HF concentration; solid-to-liquid ratio of 1:12) for ASW-Celite and ASW-Perlite.

Feedstock	Solid Raw (g)	Solid Yield (g)	Solid Yield (%)
ASW-Celite	12.64	3.16	24.99%
ASW-Perlite	12.69	6.21	48.90%

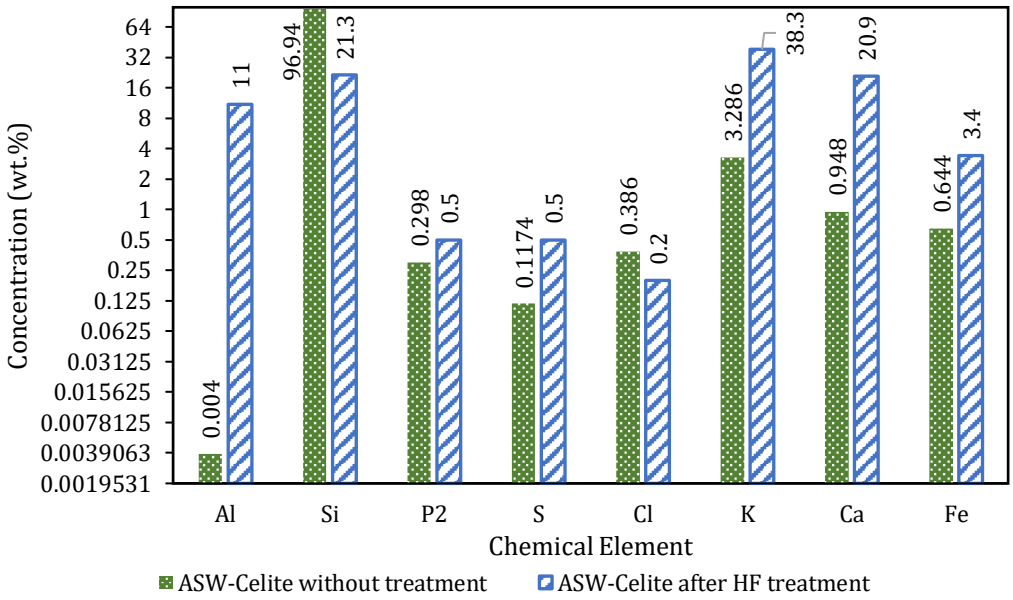

Figure 4. XRF comparison of chemical compound concentrations in ASW-Celite before and after HF treatment (10% HF concentration; solid-to-liquid ratio of 1:12).

The XRF results for raw ASW-Celite indicate that the untreated sample was overwhelmingly dominated by SiO_2, with an instrument-reported concentration of 96.94%. This finding confirms that the inorganic fraction of ASW-Celite was predominantly silica-based, consistent with the presence of Celite as the filtration aid. The marked dominance of SiO_2 accounts for the high ash content and correspondingly low fuel quality of the untreated material. Minor oxide and elemental species were also detected, including CaO, Fe_2O_3, K_2O, S, P_2O_5, Cl, and Al_2O_3.

Following HF treatment, the SiO_2 concentration decreased markedly from 96.94% to 21.30%. This represents the most significant finding from the XRF analysis and confirms the strong reactivity of HF toward silica-rich minerals. The reduction in SiO_2 is consistent with the established reaction mechanism of HF with silicate minerals, whereby HF attacks Si–O bonds to form soluble fluorosilicate species such as H_2SiF_6 [40]. Previous studies on silicate dissolution have demonstrated that HF adsorption at mineral surfaces weakens Si–O and Al–O lattice bonds, promoting the formation of fluorinated Si and Al complexes in solution [33].

Several oxide fractions increased in relative concentration following HF treatment, notably K_2O, CaO, and Al_2O_3. Specifically, K_2O increased from 3.73% to 38.30%, CaO from 9.48% to 20.90%, and Al_2O_3 from 0.004% to 11.00%. These increases are attributed to relative enrichment arising from the preferential dissolution of SiO_2. As a large proportion of silica is removed, the remaining inorganic constituents become proportionally more concentrated in the residual solid. Conversely, the decreases observed in Fe_2O_3 (from 6.44% to 3.40%), S (from 11.76% to 0.50%), and Cl (from 0.386% to 0.20%) indicate that a fraction of the iron-, sulfur-, and chlorine-containing species was also removed during leaching. Collectively, these results indicate that HF leaching was highly effective for the removal of silica, sulfur, and chlorine, while alkali and alkaline-earth mineral species were not completely eliminated.

The XRF data confirm that the primary effect of HF treatment was the selective dissolution of silica-rich mineral matter from ASW-Celite. This outcome is significant because silica is among the principal contributors to ash accumulation in biomass feedstocks and can substantially reduce fuel quality by diminishing the relative organic fraction [40], [41]. It should be noted, however, that XRF accuracy may be affected by matrix effects, sample heterogeneity, particle size, surface roughness, and variations in organic-to-inorganic composition before and after leaching [42]. Accordingly, XRF results are treated as supplementary data in the present study, with ICP-MS providing the primary quantitative basis for elemental analysis of selected elements.

3.3. ICP-MS element detection results

ICP-MS was employed to evaluate the redistribution and removal of trace, environmentally relevant, and ash-forming elements in ASW before and after HF leaching. The measured

concentrations are reported in ppb and were interpreted in conjunction with the solid-yield data to determine elemental removal efficiency, calculated according to Equation (3). ICP-MS analysis was conducted on both ASW-Celite and ASW-Perlite, for untreated samples and HF-leached samples alike.

The ICP-MS results indicate substantial removal of several toxic and environmentally relevant elements following HF leaching. In both ASW-Celite and ASW-Perlite, Cr, Ni, Cu, Zn, and Cd exhibited high removal efficiencies, as summarized in Table 4. These results demonstrate that HF leaching was effective not only for the dissolution of silica-rich mineral matter but also for the reduction of trace metals associated with the inorganic fraction of ASW.

The high removal efficiencies observed for Cu, Zn, Ni, and Cd suggest that these elements were predominantly present in acid-soluble, exchangeable, or weakly mineral-bound forms. Under acid leaching conditions, such species can be mobilized through proton-promoted dissolution, ion exchange, and complexation reactions. Analogous behavior has been reported in biomass pretreatment studies, wherein acid washing and leaching were shown to remove inorganic species and improve fuel quality by reducing ash-forming and environmentally sensitive elements [27], [28], [43].

The major mineral and ash-forming elements exhibited element-specific removal behavior following HF leaching. The removal efficiencies of Na, Mg, P, S, Cl, Ca, Mn, and Fe in ASW-Celite and ASW-Perlite are presented in Table 5. Overall, inorganic element removal was more pronounced in ASW-Celite than in ASW-Perlite, which is consistent with the lower solid yield of ASW-Celite after HF treatment. The preferential removal of S and Cl is of particular significance for bioenergy applications, as chlorine- and sulfur-containing species are commonly associated with corrosion, acid gas formation, and operational instability during combustion, pyrolysis, and gasification [41], [43]. By contrast, Ca and Mg exhibited only moderate to low removal efficiencies, particularly in ASW-Perlite. This behavior may be attributed to the formation or retention of sparingly soluble fluoride phases, such as CaF_2 or MgF_2, or to their association with more chemically resistant aluminosilicate minerals. The comparatively lower removal of Mg and Ca in ASW-Perlite further supports the interpretation that perlite-derived aluminosilicate structures are more resistant to HF attack than the amorphous silica characteristic of Celite.

Table 4. Concentrations of toxic and environmentally relevant elements in ASW before and after HF leaching (10% HF concentration; solid-to-liquid ratio of 1:12).

Elements	ASW-Celite			ASW-Perlite		
	Concentration (ppb)		Removal efficiency (%)	Concentration (ppb)		Removal efficiency (%)
	ASW without treatment	ASW after HF treatment		ASW without treatment	ASW after HF treatment	
Be	0.290	N/A	-	0.029	N/A	-
Cr	96.335	104.928	73%	191.82	73.911	81%
Ni	45.131	15.810	91%	58.731	15.127	87%
Cu	101.969	34.187	92%	86.56	12.827	93%
Zn	178.732	43.962	94%	126.164	30.011	88%
As	5.000	N/A	-	8.333	N/A	-
Se	22.000	N/A	-	10	N/A	-
Mo	4.488	N/A	-	3.088	N/A	-
Cd	0.287	0.161	86%	0.405	0.051	94%
Sb	0.410	1.345	18%	0.098	0.119	41%
Hg	0.199	0.459	42%	0.242	N/A	-
Tl	0.330	1.261	4%	16.368	N/A	-
Pb	14.097	N/A	-	5.286	N/A	-
Th	10.019	N/A	-	2.581	N/A	-
U	1.311	N/A	-	0.029	N/A	-

[1] N/A indicates “Not Available”.

Table 5. Concentrations of major mineral and ash-forming elements in ASW-Celite and ASW-Perlite before and after HF leaching (10% HF concentration; solid-to-liquid ratio of 1:12).

Elements	ASW-Celite			ASW-Perlite		
	Concentration (ppb)		Removal efficiency (%)	Concentration (ppb)		Removal efficiency (%)
	ASW without treatment	ASW after HF treatment		ASW after HF treatment	ASW after HF treatment	
C	4,047.201	16,189.794	0.02%	6,333.543	9851.633	24%
N	3,823,721.8	3,975,015.924	74%	3,085,661	4527216	28%
Na	10,484.575	13,775.785	67%	12,628.780	11918.85	54%
Mg	3,501.528	4,922.386	65%	9,380.213	14669.95	24%
Al	23,870.651	N/A	-	10,606.290	N/A	-
Si	3,757.929	N/A	-	4,538.064	N/A	-
P	753.069	233.554	92%	270.585	162.147	71%
S	789.845	148.304	95%	942.965	0	100%
Cl	50.278	0	100%	122.154	0	100%
K	2,393.107	N/A	-	2,868.874	N/A	-
Ca	2,221.439	4,290.894	52%	3,272.920	4751.896	29%
Mn	784.410	1,705.751	80%	1,958.434	1127.014	72%
Fe	2,130.698	11,014.242	62%	3,671.731	4397.703	41%

[1] N/A indicates "Not Available".

It is acknowledged that the ICP-MS results are subject to inherent methodological limitations in the context of the present study. Accordingly, ICP-MS data are treated as supporting evidence for elemental removal and are interpreted in conjunction with XRF, proximate analysis, FTIR, and solid-yield results to provide a comprehensive assessment.

3.4. FTIR analysis of ASW before and after HF leaching

FTIR spectra of untreated and HF-treated ASW samples were recorded in ATR mode over the wavenumber range of 4000–400 cm^{-1} to evaluate changes in organic functional groups and silica-related mineral phases, as presented in Figure 5.

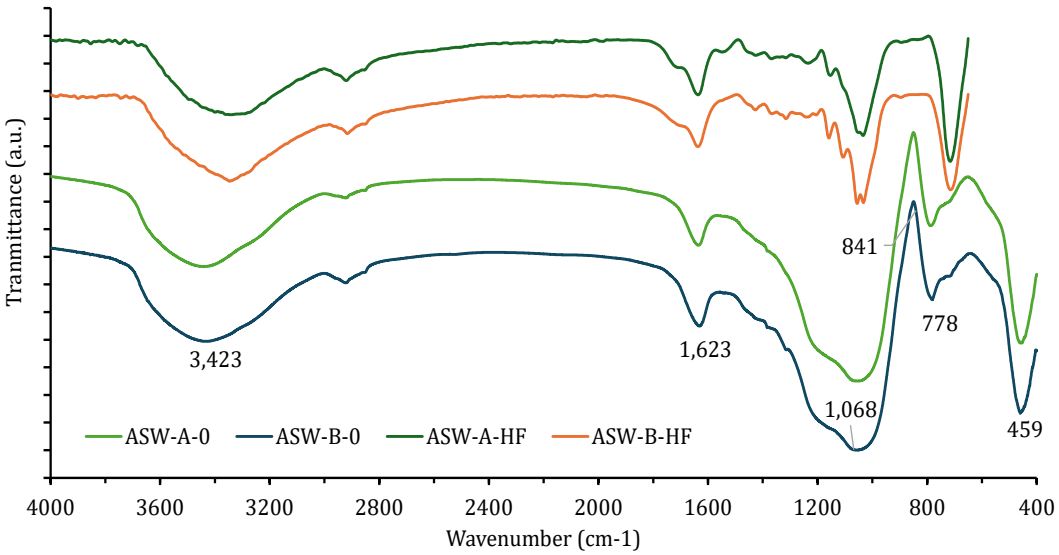

Figure 5. FTIR spectra of ASW-Celite (ASW-A) and ASW-Perlite (ASW-B) before (ends with 0) and after HF leaching (10% HF concentration; solid-to-liquid ratio of 1:12).

The broad absorption band observed at approximately 3300 cm^{-1} in all samples is assigned to O–H stretching vibrations. This feature is commonly associated with hydroxyl-containing biomass constituents, particularly polysaccharide residues, and may also incorporate contributions from adsorbed water and surface silanol groups. In agar and *Gracilaria*-derived materials, O–H stretching in the 3300–3400 cm^{-1} region is characteristic of hydroxyl-rich carbohydrate structures [1], [2]. The persistence of this band following HF treatment indicates that hydroxyl-containing organic structures were retained in the solid residue after leaching. An additional aliphatic C–H stretching band at approximately 2925 cm^{-1} further corroborates the presence of residual organic matter [44]. The absorption band at approximately 1600 cm^{-1} is attributed to O–H bending vibrations of adsorbed or structurally bound water, a feature commonly observed in hydroxyl-rich biomass and polysaccharide-based materials, including agarocolloid-type constituents [45].

By contrast, strong absorption bands at approximately 1060, 840, 778, and 453 cm^{-1} are assigned to Si–O–Si stretching and bending vibrations, confirming a substantial silica contribution to the inorganic fraction [46]. The band at approximately 1630 cm^{-1} is attributed to the bending mode (δ O–H) of coordinated molecular water [46]. These spectral features are consistent with previously reported FTIR spectra of perlite and of solid waste derived from agar processing facilities [1]. The elevated intensity of the Si–O–Si bands in untreated ASW, and their marked attenuation following HF treatment, are in good agreement with the XRF results, which indicate a pronounced reduction in SiO_2 concentration after leaching. This concordance between spectroscopic and compositional data confirms that silica-rich phases — originating from Celite in ASW-Celite and perlite in ASW-Perlite — dominated the inorganic fraction of the raw material. After HF leaching, the intensity of the Si–O–Si bands decreased markedly in both sample types, most notably at approximately 1060, 840, and 778 cm^{-1}, providing direct spectroscopic evidence of silica dissolution.

3.5. Ultimate and proximate analysis

The ultimate composition, proximate analysis, and HHV results for ASW before and after HF leaching are presented in Table 6. These results collectively highlight the dominant role of inorganic constituents in governing the physicochemical and energy properties of ASW, and the extent to which demineralization modifies these characteristics.

The proximate analysis reveals that untreated ASW was dominated by inorganic matter. ASW-Celite contained 85.84 wt% ash, while ASW-Perlite contained 77.10 wt% ash. These values are substantially higher than those typically reported for conventional lignocellulosic biomass [29]. Comparable challenges have been documented for agar-processing solid waste, wherein the presence of inorganic filtration residues severely limits direct biomass valorization [1].

Following HF leaching, ash content decreased markedly in both sample types, as shown in Table 7. ASW-Celite-HF retained 44.99 wt% ash, while ASW-Perlite-HF retained 24.83 wt% ash. The corresponding ash removal efficiencies were 38.94% for ASW-Celite and 58.23% for ASW-Perlite, as detailed in Table 8. The more pronounced reduction observed in ASW-Perlite indicates that HF leaching substantially diminished the inorganic burden associated with perlite-containing ASW. Nevertheless, HF leaching did not fully convert the treated residue into a material comparable to conventional biomass fuel, confirming that demineralization is a necessary but potentially insufficient pretreatment step for silica-rich ASW.

The ultimate analysis further confirms that HF leaching enriched the organic fraction of ASW. Carbon content increased appreciably in both sample types following treatment, a consequence of the relative concentration of organic constituents upon partial removal of mineral matter. Since oxygen content was calculated by difference, this increase also reflects the relative enrichment of oxygenated organic structures following ash removal. The persistently high oxygen content indicates that the treated samples remained highly oxygenated and had not undergone carbonization or deoxygenation — behavior that is consistent with the selective nature of HF leaching, which removes inorganic mineral phases without thermochemically modifying the biomass structure.

The H/C and O/C atomic ratios derived from the ultimate analysis further support this interpretation, as depicted in the Van Krevelen diagram in Figure 6. The Van Krevelen diagram illustrates the evolution of elemental composition following HF leaching and is widely employed to evaluate biomass composition and thermochemical transformation pathways [14]. *Gracilaria sp.* (GRA), the algal feedstock processed by the agar extraction plant, lies within the typical carbohydrate biomass region (H/C ≈ 2.0; O/C ≈ 1.0), while untreated ASW samples are positioned in proximity but are slightly displaced due to dilution of the organic

Table 6. Elemental (C, H, N, S, O) and Proximate compositions of ASW before and after HF leaching (10% HF concentration; solid-to-liquid ratio of 1:12).

Properties	ASW-Celite	ASW-Perlite	ASW-Celite-HF	ASW-Perlite-HF
C	4.69	9.83	12.52	16.1
H	1.26	1.7	5.45	3.5
N	N/D[1]	0.29	0.91	1.57
S	0.03	N/D	0	0
O	8.9	11.09	36.12	54
MC	2.74	4.89	N/A[2]	N/A
VM	9.05	27.78	N/A	N/A
Ash	85.84	77.1	44.99	24.83
FC	2.37	3.46	N/A	N/A
HHV (MJ/kg)	1.91	4.8	6.52	3.19

C, H, N, S, O are reported in wt%.
MC (moisture content), VM (volatile matter), ash content, and FC (fixed carbon) were reported in wt%.
[1] N/D indicates "Not Detected".
[2] N/A indicates "Not Available".

Table 7. Ash content, ash removal efficiency, and mass balance of HF-leached ASW (10% HF concentration; solid-to-liquid ratio of 1:12), reported in wt%.

Biomass	Treatment	Ash Content (wt%)	Ash Removal Efficiency (%)	Mass Balance (%)	
				Ash Retained	Ash Removed
ASW-Celite	No treatment	85.84	-	-	-
ASW-Perlite	No treatment	77.1	-	-	-
ASW-Celite-HF	HF leaching	44.99	38.943	52.411	33.429
ASW-Perlite-HF	HF leaching	24.83	58.230	32.205	44.895

fraction by silica-rich inorganic components. Both H/C and O/C ratios increased in ASW-Celite and ASW-Perlite following HF treatment. The relatively elevated O/C ratios in the treated samples may indicate the retention of residual soluble inorganic species within the solid matrix, suggesting that supplementary washing steps could further reduce inorganic content. This is consistent with prior studies demonstrating that acid leaching followed by adequate rinsing enhances mineral removal efficiency, as soluble and weakly bound inorganic species may remain entrapped in the solid matrix in the absence of sufficient washing [47]. The H/C and O/C values of the treated samples remain higher than those characteristic of carbonized solid fuels — materials in which fuel densification has proceeded via dehydration or decarboxylation. This observation implies that improvement in fuel quality requires not only ash reduction but also a reduction in oxygenated functional group content. Accordingly, further thermochemical upgrading — such as hydrothermal carbonization, torrefaction, or pyrolysis — would be expected to reduce H/C and O/C ratios and improve the energy density of the treated material [40], [41], [48].

The HHV results indicate that HF leaching improved the energy content of ASW-Celite but not ASW-Perlite. The HHV of ASW-Celite increased from 1.91 MJ kg^{-1} to 6.52 MJ kg^{-1}, representing a net gain of 4.61 MJ kg^{-1}. This improvement is consistent with the substantial reduction in ash content and the concurrent increase in carbon and hydrogen concentrations. By contrast, the HHV of ASW-Perlite decreased from 4.80 MJ kg^{-1} to 3.19 MJ kg^{-1} following HF treatment, despite reductions in ash content and increases in carbon content. This apparent anomaly is explained by the very high oxygen content of ASW-Perlite-HF (54 wt%). In the HHV correlation of Equation (4), carbon and hydrogen contribute positively to the calculated heating value, whereas oxygen and nitrogen exert a negative influence. Consequently, the increase in carbon content was insufficient to offset the strong negative contribution of the elevated oxygen fraction in ASW-Perlite-HF.

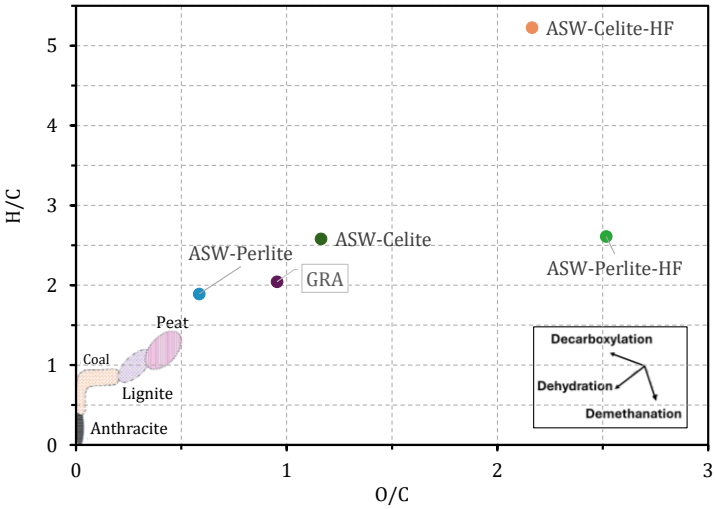

Figure 6. Van Krevelen diagram of untreated ASW and ASW after HD leaching with 10% concentration and with a solid-to-liquid ratio 1:12.

Relative to conventional lignocellulosic biomass fuels, which typically exhibit HHV values in the range of 15–20 MJ kg^{-1}, the energy content of both treated ASW samples remains low: ASW-Celite-HF reached 6.52 MJ kg^{-1} and ASW-Perlite-HF reached only 3.19 MJ kg^{-1}. These results indicate that further thermochemical upgrading — such as hydrothermal carbonization, torrefaction, or pyrolysis — would be required prior to deployment in energy applications.

4. Conclusions

This study demonstrated that hydrofluoric acid (HF) leaching at a concentration of 10% and a solid-to-liquid ratio of 1:12 constitutes an effective pretreatment strategy for reducing the silica-rich mineral fraction in agar solid waste (ASW) — a material in which silica originates from filtration aids introduced during the agar extraction process. XRF, ICP-MS, and FTIR analyses collectively confirmed that HF leaching selectively targeted silica-rich mineral phases derived from these filtration aids. ICP-MS analysis further demonstrated the reduction of several ash-forming and environmentally relevant elements, including Cr, Ni, Cu, Zn, Cd, P, S, Cl, Mn, and Fe, with toxic and environmentally sensitive species such as Cr, Ni, Cu, Zn, and Cd exhibiting particularly high removal efficiencies in both ASW-Celite and ASW-Perlite. HF leaching transformed ASW-Celite — which contains Celite as the filtration aid — from a highly silica-dominated residue into a material with substantially reduced SiO_2 content. The SiO_2 concentration decreased from 96.94% to 21.30%, and the solid yield decreased to 24.99%, confirming extensive dissolution of the silica-rich fraction. By comparison, ASW-Perlite — which contains perlite — retained 48.90% of its initial mass, indicating lower demineralization efficiency attributable to the greater chemical resistance of aluminosilicate-based mineral structures. Untreated ASW was characterized by exceptionally high ash content: 85.84 wt% in ASW-Celite and 77.10 wt% in ASW-Perlite. Following HF leaching, ash content decreased to 44.99 wt% in ASW-Celite-HF and 24.83 wt% in ASW-Perlite-HF, confirming substantial demineralization in both cases. Ultimate analysis demonstrated that demineralization increased the relative organic fraction of ASW, with carbon content increasing from 4.69 wt% to 12.52 wt% in ASW-Celite and from 9.83 wt% to 16.10 wt% in ASW-Perlite. The energy response, however, differed between the two sample types. The HHV of ASW-Celite increased from 1.91 MJ kg^{-1} to 6.52 MJ kg^{-1}, reflecting improved fuel quality following mineral removal. By contrast, the HHV of ASW-Perlite decreased from 4.80 MJ kg^{-1} to 3.19 MJ kg^{-1}, primarily due to the elevated oxygen content of the treated residue. This outcome demonstrates that ash reduction alone is insufficient to guarantee energy improvement when the residual organic fraction remains highly oxygenated. Although HF leaching improved the physicochemical properties of ASW, the residual ash content, high oxygen concentration, and low HHV values indicate that further upgrading is required prior to direct utilization as a solid biofuel. Future investigations should address the optimization of acid concentration, washing intensity, and solid-to-liquid ratio, as well as the integration of HF leaching with thermochemical deoxygenation processes — such as torrefaction, hydrothermal carbonization, or pyrolysis — to further enhance fuel quality and advance the practical valorization of ASW.

Acknowledgements

The authors gratefully acknowledge the financial support provided by the Ministry of Higher Education and the Ministry of Finance of Indonesia through the BPI and LPDP program. Additional financial support from Universitas Mercu Buana is also sincerely appreciated. The authors would like to thank the Surfactant and Bioenergy Research Center (SBRC)-IPB University for providing research facilities. Appreciation is also extended to Universiti Kebangsaan Malaysia and Badan Riset dan Inovasi Nasional (BRIN) for their support in characterization and analytical facilities. The authors also sincerely thank Muhamad Fiqri and Wahyu Hasan Latudi for their assistance with material preparation.

Declaration of Generative AI and AI-Assisted Technologies in the Writing Process

The authors used ChatGPT and Claude to assist in improving the English language, refining the organization and clarity of the manuscript. All AI-assisted content was critically reviewed, revised, and validated by the authors against the original experimental data and relevant scientific literature. The authors take full responsibility for the scientific accuracy, originality, and integrity of the manuscript, in accordance with the guidelines of the Committee on Publication Ethics (COPE).

References

[1] M. Muryanto *et al*., "Characterization of solid waste biomass of agar processing plants and scale-up production of bioethanol," *Biomass Convers. Biorefin.*, vol. 14, no. 18, pp. 22357–22366, 2024, doi: 10.1007/s13399-023-04464-7.

[2] F. S. Tadeo *et al*., "Biochemical profiling of *Gracilaria edulis* agar waste for aquaculture applications," *Egypt. J. Aquat. Biol. Fish.*, vol. 29, no. 4, pp. 3139–3156, Jul. 2025, doi: 10.21608/EJABF.2025.449750.

[3] J. Basmal, I. Munifah, M. Rimmer, and N. Paul, "Identification and characterization of solid waste from *Gracilaria* sp. extraction," *IOP Conf. Ser. Earth Environ. Sci.*, vol. 404, no. 1, Art. no. 012057, Jan. 2020, doi: 10.1088/1755-1315/404/1/012057.

[4] I. Munifah, J. Basmal, R. Kusumawati, and H. E. Irianto, "Cellulase derived from *Chryseobacterium indologenes* LA4K isolated from Indonesian agar-agar industry solid waste," *IOP Conf. Ser. Earth Environ. Sci.*, vol. 462, no. 1, Art. no. 012007, Mar. 2020, doi: 10.1088/1755-1315/462/1/012007.

[5] A. O. L. Siang, A. M. Leman, D. Feriyanto, S. S. Abdulmalik, and S. Zakaria, "Sustainable biodiesel production from waste cooking oil and crude palm oil using a custom mini pilot plant," *Int. J. Innov. Mech. Eng. Adv. Mater.*, vol. 6, no. 1, pp. 7–21, Aug. 2024, doi: 10.22441/ijimeam.v6i1.23734.

[6] E. Agustian, A. Praptijanto, D. Sebayang, A. Z. M. Rus, and S. Hasan, "Biodiesel production from waste cooking oil by using ultrasonic tubular reactor," *Int. J. Innov. Mech. Eng. Adv. Mater.*, vol. 2, no. 1, pp. 31–38, 2016, doi: 10.22441/ijimeam.v2i1.18955.

[7] M. A. M. Sidik, A. M. Leman, D. Feriyanto, S. S. Abdulmalik, and S. Zakaria, "Green technology for sustainable agriculture: Bio-fertilizer production from municipal waste to preserve the environment," *Int. J. Innov. Mech. Eng. Adv. Mater.*, vol. 5, no. 3, pp. 118–124, Jan. 2024, doi: 10.22441/ijimeam.v5i3.23743.

[8] G. Wangge, Y. V. Servianus, and T. Rande, "Utilization of plastic waste and rice husk ash in polyethylene-based composites for ceiling applications," *Int. J. Innov. Mech. Eng. Adv. Mater.*, vol. 7, no. 3, pp. 162–172, Jan. 2026, doi: 10.22441/ijimeam.v7i3.36658.

[9] D. A. Roberts, N. A. Paul, S. A. Dworjanyn, Y. Hu, M. I. Bird, and R. de Nys, "*Gracilaria* waste biomass (sampah rumput laut) as a bioresource for selenium biosorption," *J. Appl. Phycol.*, vol. 27, pp. 611–620, 2015, doi: 10.1007/s10811-014-0346-y.

[10] I. Munifah and H. E. Irianto, "Characteristics of solid waste agar industries," *Squalen Bull. Mar. Fish. Postharvest Biotechnol.*, vol. 13, no. 3, pp. 125–132, Dec. 2018, doi: 10.15578/squalen.v13i3.292.

[11] K. Srivastava, N. Shringi, V. Devra, and A. Rani, "Pure silica extraction from perlite: Its characterization and affecting factors," *Int. J. Innov. Res. Sci. Eng. Technol.*, vol. 2, no. 7, pp. 2936–2942, 2013.

[12] A. Pourjavadi, R. Soleyman, H. Ghasemzadeh, and H. Salimi, "CMC/Celite superabsorbent composites: Effect of reaction variables on saline-absorbency under load," *Iran. Polym. J.*, vol. 19, no. 8, pp. 571–579, 2010.

[13] M. T. Phong, T. D. Hai, and P. D. Tuan, "Effects of fluxing agents on filter aids prepared from Lam-Dong diatomate," *ASEAN J. Chem. Eng.*, vol. 12, no. 2, pp. 27–34, 2012, doi: 10.22146/ajche.49740.

[14] V. S. Ekanthalu, S. Narra, T. Ender, E. Antwi, and M. Nelles, "Influence of post- and pre-acid treatment during hydrothermal carbonization of sewage sludge on P-transformation and the characteristics of hydrochar," *Processes*, vol. 10, no. 1, Art. no. 151, Jan. 2022, doi: 10.3390/pr10010151.

[15] P. F. Pratt, "Digestion with hydrofluoric and perchloric acids for total potassium and sodium," in *Methods of Soil Analysis, Part 2: Chemical and Microbiological Properties*, C. A. Black, Ed. Madison, WI, USA: American Society of Agronomy, 1965, pp. 1019–1021, doi: 10.2134/agronmonogr9.2.c19.

[16] R. G. Ayvazyan and K. Jacoby, "Kinetics and spectroscopic characterization of silica nanoparticles formed while etching quartz in hydrofluoric acid," *Mater. Chem. Phys.*, vol. 305, Art. no. 127881, Sep. 2023, doi: 10.1016/j.matchemphys.2023.127881.

[17] A. S. Buravtsov, D. E. Vernigora, O. V. Olender, A. V. Gladkov, M. V. Tryapyshko, and B. V. Grigorev, "Organic mud acid implementation in Western Siberian reservoir condition as an alternative to regular mud acid," *Neftyanoe Khozyaystvo—Oil Ind.*, vol. 2023, no. 9, pp. 123–127, 2023, doi: 10.24887/0028-2448-2023-9-123-127.

[18] T. R. Mandula and R. Srinivasan, "Electrochemical impedance spectroscopic studies on niobium anodic dissolution in HF," *J. Solid State Electrochem.*, vol. 21, no. 11, pp. 3155–3167, 2017, doi: 10.1007/s10008-017-3634-z.

[19] P. Crook, N. S. Meck, and R. B. Rebak, "The influence of composition upon surface degradation and stress corrosion cracking of the Ni-Cr-Mo alloys in wet hydrofluoric acid," *NACE Int. Corros. Conf. Ser.*, Paper C2007-07481, pp. 1–13, 2007, doi: 10.5006/C2007-07481/53715.

[20] I. Vlastelic and J. Piro, "Volatilisation of trace elements during evaporation to dryness of HF-dissolved silicates (BHVO-2, AGV-1, BIR-1, UB-N): Open- versus closed-system conditions," *Geostand. Geoanal. Res.*, vol. 46, no. 3, pp. 519–534, Sep. 2022, doi: 10.1111/ggr.12428.
[21] D. V. Yusupov *et al*., "Fluorite formation in poplar leaves (*Populus balsamifera* L.) in an HF-polluted area," *Water Air Soil Pollut.*, vol. 232, no. 9, Art. no. 369, 2021, doi: 10.1007/s11270-021-05279-w.
[22] A. L. Bezerra de Oliveira *et al*., "Hydrofluoric acid-free digestion of geological samples for the quantification of rare earth elements by inductively coupled plasma-optical emission spectrometry," *Geostand. Geoanal. Res.*, vol. 43, no. 4, pp. 689–699, Dec. 2019, doi: 10.1111/ggr.12286.
[23] Q. Guan *et al*., "Acidic constant of hydrofluoric acid in high-pressure and high-temperature geofluids," *ACS Earth Space Chem.*, vol. 10, no. 2, pp. 319–327, Feb. 2026, doi: 10.1021/acsearthspacechem.5c00224.
[24] Y. Yang, C. Lan, Y. Wang, Z. Zhao, and B. Li, "Recycling of ultrafine NdFeB waste by the selective precipitation of rare earth and the electrodeposition of iron in hydrofluoric acid," *Sep. Purif. Technol.*, vol. 230, Art. no. 115870, Jan. 2020, doi: 10.1016/j.seppur.2019.115870.
[25] K. G. W. Inn, "Geochemistry of resistates: The last word?," *J. Radioanal. Nucl. Chem.*, vol. 318, no. 1, pp. 767–776, 2018, doi: 10.1007/s10967-018-6123-7.
[26] R. W. Schutz, S. Hernandez, and H. W. Walker, "Effective inorganic salt corrosion inhibitors for titanium components exposed to dilute hydrofluoric acid well stimulation fluids," *NACE Int. Corros. Conf. Ser.*, vol. 2, pp. 1054–1066, 2017.
[27] H. Hörhammer, C. Dou, R. Gustafson, A. Suko, and R. Bura, "Removal of non-structural components from poplar whole-tree chips to enhance hydrolysis and fermentation performance," *Biotechnol. Biofuels*, vol. 11, no. 1, Art. no. 222, 2018, doi: 10.1186/s13068-018-1219-4.
[28] A. Saddawi, J. M. Jones, A. Williams, and C. Le Coeur, "Commodity fuels from biomass through pretreatment and torrefaction: Effects of mineral content on torrefied fuel characteristics and quality," *Energy Fuels*, vol. 26, no. 11, pp. 6466–6474, Nov. 2012, doi: 10.1021/ef2016649.
[29] A. Sudarma *et al*., "Influence of inorganic content on hydrochar quality from high-ash agar extraction waste via hydrothermal carbonization," *SINERGI*, 2026, doi: 10.22441/sinergi.2026.3.001.
[30] I. Hamidu, B. Afotey, B. Kwakye-Awuah, and D. A. Anang, "Synthesis of silica and silicon from rice husk feedstock: A review," *Heliyon*, vol. 11, no. 4, Art. no. e42491, Feb. 2025, doi: 10.1016/j.heliyon.2025.e42491.
[31] R. B. Carpio, Y. Zhang, C.-T. Kuo, W.-T. Chen, L. C. Schideman, and R. L. de Leon, "Characterization and thermal decomposition of demineralized wastewater algae biomass," *Algal Res.*, vol. 38, Art. no. 101399, Mar. 2019, doi: 10.1016/j.algal.2018.101399.
[32] R. Febrianto, Sudarno, and R. Kusdarwati, "The effect of demineralization stage of agar's solid waste on the characterization of activated carbon," *IOP Conf. Ser. Earth Environ. Sci.*, vol. 236, no. 1, Art. no. 012033, Mar. 2019, doi: 10.1088/1755-1315/236/1/012033.
[33] G. Rosales, M. Ruiz, and M. Rodriguez, "Study of the extraction kinetics of lithium by leaching β-spodumene with hydrofluoric acid," *Minerals*, vol. 6, no. 4, Art. no. 98, Sep. 2016, doi: 10.3390/min6040098.
[34] W. E. Kline and H. S. Fogler, "Dissolution of silicate minerals by hydrofluoric acid," *Ind. Eng. Chem. Fundam.*, vol. 20, no. 2, pp. 155–161, May 1981, doi: 10.1021/i100002a008.
[35] W. Wu *et al*., "Experimental research on deep silicon removal in spent SCR catalysts," *Processes*, vol. 12, no. 2, Art. no. 290, Feb. 2024, doi: 10.3390/pr12020290.
[36] W. Zha, B. Lin, W. Yang, T. Liu, T. Liu, and W. Wang, "Mineral dissolution and wettability evolution in coal acidization: Molecular mechanisms of hydrophobic transformation," *Energy Fuels*, vol. 39, no. 23, pp. 11031–11040, Jun. 2025, doi: 10.1021/acs.energyfuels.5c01931.
[37] Y. Zhao *et al*., "Water–HCl sequential leaching of waste barrier material from aluminum electrolysis cell," *Materials*, vol. 18, no. 8, Art. no. 1748, Apr. 2025, doi: 10.3390/ma18081748.
[38] A. Demirbas and M. F. Demirbas, "Biodiesel from algae," in *Algae Energy*, Green Energy and Technology. London, U.K.: Springer, 2010, pp. 139–157, doi: 10.1007/978-1-84996-050-2_6.
[39] Ö. Bilgin, H. Hacıfazlıoğlu, and D. Sert, "Leaching of coal by trioxoboric acid for coal cleaning," *Physicochem. Probl. Miner. Process.*, vol. 57, no. 5, pp. 129–136, 2021, doi: 10.37190/ppmp/141489.
[40] L. Puri, Y. Hu, and G. Naterer, "Critical review of the role of ash content and composition in biomass pyrolysis," *Front. Fuels*, vol. 2, Art. no. 1378361, Mar. 2024, doi: 10.3389/ffuel.2024.1378361.
[41] P. Giudicianni *et al*., "Inherent metal elements in biomass pyrolysis: A review," *Energy Fuels*, vol. 35, no. 7, pp. 5407–5478, Apr. 2021, doi: 10.1021/acs.energyfuels.0c04046.
[42] F. Endriss *et al*., "Evaluation and optimization of an X-ray fluorescence analyzer for rapid analysis of chemical elements in solid biofuels," *Energy Fuels*, vol. 38, no. 17, pp. 16426–16440, Sep. 2024, doi: 10.1021/acs.energyfuels.4c01771.
[43] Q. Liu, S. C. Chmely, and N. Abdoulmoumine, "Biomass treatment strategies for thermochemical conversion," *Energy Fuels*, vol. 31, no. 4, pp. 3525–3536, Apr. 2017, doi: 10.1021/acs.energyfuels.7b00258.
[44] O. Farobie *et al*., "Valorization of *Ulva lactuca* via hydrothermal carbonization: Effects of temperature, time, and concentration on hydrochar," *J. Pengolah. Has. Perikan. Indones.*, vol. 29, no. 2, pp. 161–177, 2026, doi: 10.17844/f3kztf96.
[45] A. Nadri *et al*., "The invasive seaweed *Agarophyton vermiculophyllum* from Oualidia Lagoon (northwestern Moroccan Atlantic coast) as a source of agar: Yield, chemical characteristics, and rheological properties," *J. Mar. Sci. Eng.*, vol. 11, no. 9, Art. no. 1696, Aug. 2023, doi: 10.3390/jmse11091696.
[46] Z. Zujovic, W. V. K. Wheelwright, P. A. Kilmartin, J. V. Hanna, and R. P. Cooney, "Structural investigations of perlite and expanded perlite using ^{1}H, ^{27}Al, and ^{29}Si solid-state NMR," *Ceram. Int.*, vol. 44, no. 3, pp. 2952–2958, Feb. 2018, doi: 10.1016/j.ceramint.2017.11.047.
[47] S. B. Liaw and H. Wu, "Leaching characteristics of organic and inorganic matter from biomass by water: Differences between batch and semi-continuous operations," *Ind. Eng. Chem. Res.*, vol. 52, no. 11, pp. 4280–4289, Mar. 2013, doi: 10.1021/ie3031168.
[48] J. Petrović, M. Simić, M. Mihajlović, M. Koprivica, M. Kojić, and I. Nuić, "Upgrading fuel potentials of waste biomass via hydrothermal carbonization: Original scientific paper," *Hem. Ind.*, vol. 75, no. 5, pp. 297–305, Oct. 2021, doi: 10.2298/HEMIND210507025P.